Origin of the quasi-universality of the graphene minimal conductivity

J. J. Palacios[1]

[1]*Departamento de Física de la Materia Condensada, Universidad Autónoma de Madrid, Cantoblanco, Madrid 28049, Spain*

It is a fact that the minimal conductivity σ_0 of most graphene samples is larger than the well-established universal value for ideal graphene $4e^2/\pi h$; in particular, larger by a factor $\gtrsim \pi$. Despite intense theoretical activity, this fundamental issue has eluded an explanation so far. Here we present fully atomistic quantum mechanical estimates of the graphene minimal conductivity where electron-electron interactions are considered in the framework of density functional theory. We show the first conclusive evidence of the dominant role on the minimal conductivity of charged impurities over ripples, which have no visible effect. Furthermore, in combination with the logarithmic scaling law for diffusive metallic graphene, we ellucidate the origin of the ubiquitously observed minimal conductivity in the range $8e^2/h > \sigma_0 \gtrsim 4e^2/h$.

PACS numbers: 72.80.Vp,73.22.Pr,72.15.Rn

I. INTRODUCTION

The ensuing years after the first reported transport measurements of isolated graphene flakes have witnessed an intense debate on the origin of the *quasi*-universal value of the minimal conductivity σ_0. The fact that experimental confirmations of the celebrated universal minimal conductivity $4e^2/\pi h$, expected for ideal graphene, are the exception[1,2] rather than the rule and that most graphene samples present larger values, typically $\gtrsim 4e^2/h$, regardless of varying experimental conditions[3–8], remains one the major fundamental unresolved questions in graphene physics. Although this issue has spurred a vast amount of theoretical work[9–19,21–23], to date, the answer remains elusive and no theory has been able to render a full picture of this jigsaw puzzle.

Numerical[9,10] as well as analytical work[11] for simple models of disorder and non-interacting electrons indicate that, as long as intervalley scattering is avoided, single-parameter scaling applies. This means that a beta function $\beta(\sigma_0) = d\mathrm{Ln}(\sigma_0)/d\mathrm{Ln}(L)$ exists, where L is the size of the sample. In particular, $\beta(\sigma_0) > 0$, behaving as $1/(\pi\sigma_0)$ for $\sigma_0 \to \infty$. In other words, neutral graphene would not present a metal-insulator transition, being its conductivity bounded from below by the universal value $\sigma_0 = 4e^2/\pi h$ for ideal graphene and unbounded from above ($\sigma_0 \to \infty$) as the disorder is increased. This prediction ultimately relies on the expectation that intervalley scattering is not activated for most common types of (long-ranged) disorder and relevant length scales, a fact confirmed by some atomistic simulations[12], but questioned by others[13].

Alternatively, there have been efforts to consider likely sources of disorder such as nearby charged impurities[14–17], ripples[21], and resonant scatterers[22] in the most possible realistic manner. This usually comes at the expense of a rigourous quantum mechanical treatment of transport which renders σ_0 size independent[14,15,21–23]. A number of predictions can be made in these semiclassical aproaches, having in common, e.g., the fact that σ_0 always decreases with increasing impurity concentration n_{imp} in addition to not being bounded from above as $n_{\mathrm{imp}} \to 0$. This is at odds with the theoretical predictions mentioned in the previous paragraph and hardly agrees with available experimental evidence[3–8]. The inherent limitations of semiclassical approaches have been recently appreciated[18,19] and are at the heart of the discrepancy. One cannot deny, however, the insight gained on the actual microscopic origin of the minimal conductivity from a realistic treatment of disorder. Combining a full quantum mechanical approach to transport with a realistic description of disorder and screening seems to be the only way to resolve the controversy and this is our major contribution in this work.

Our findings can be summarized as follows. (i) First, our calculations corroborate previous theoretical work and agree with experimental findings such as the observed linear behavior of the conductivity with electron density as well as the observed different mobilities for electrons and holes. (ii) Second, charged impurities prevail over ripples in the experimentally relevant range of impurity concentrations and distances to the graphene flake, increasing the clean-limit conductivity. (v) Finally, this increase is limited to a small percentage of the clean-limit value for small systems, which, in combination with the logarithmic scaling law predicted in the absence of intervalley scattering, allows us to explain the narrow range of values $8e^2/h > \sigma_0 \gtrsim 4e^2/h$ of the observed graphene minimal conductivity.

II. HYDROPHENE: A MINIMAL MODEL

We consider a model for graphene where the C atoms are replaced by hydrogenic atoms. The π orbitals of the C atoms, responsible for the low energy physics, are represented by the s orbitals of the hydrogenic atoms, which, in turn, are approximated by a gaussian function. The gaussian exponent is optimized to reproduce the low-energy band structure of real graphene when both are

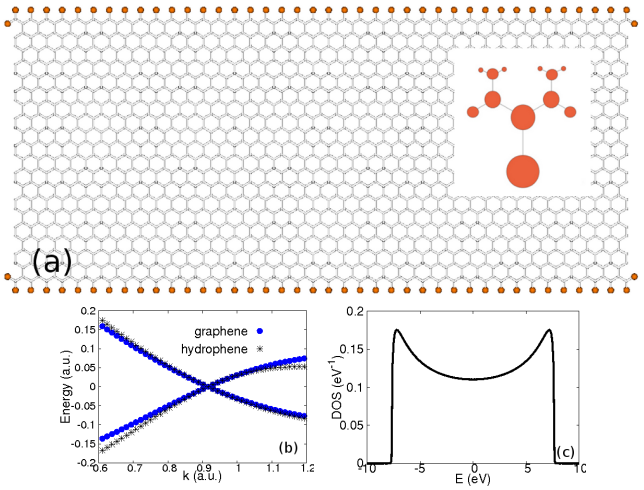

FIG. 1: Color online. (a) A hydrophene ribbon contacted to metallic electrodes as to drive the current in the armchair direction (only the first layer of the electrodes is shown). The electrodes are modeled here by a bidimensional three-fold coordinated tight-binding Bethe lattice, schematically shown in the inset. (b) Band structure (in atomic units) in the local density approximation near one of the Dirac points for graphene and hydrophene where a minimal basis set has been used for graphene. (c) Electrodes density of states per atom for a nearest-neighbors hopping amplitude $t = 2.7$ eV.

computed in the local density approximation (LDA) as implemented in GAUSSIAN03[20] [see Fig. 1(b)]. We will refer to this model as *hydrophene*. We are interested in the conductivity, defined through $\sigma = G\frac{L}{W}$, where G is the conductance of finite hydrophene ribbons of width W along the zigzag direction (x) and length L along the armchair direction (y). The latter coincides here with the direction of the current which is driven by metallic electrodes contacted along the width of the ribbons as shown in Fig. 1(a). The metallic electrodes are modeled by a bidimensional tight-binding Bethe lattice of coordination three and only nearest-neighbors hopping where the six crystallographic directions coincide with those of the ribbon (see inset). This electrode model relates closely to graphene, but presents a finite density of states at the neutrality point $E = 0$ [see Fig. 1(c)]. As shown in Fig. 1(a), a branch of the Bethe lattice is connected to each undercoordinated atom on the zigzag edge. The minimal conductivity (defined in the limit $W/L \to \infty$) depends on the particular choice for the electrode model, but never exceeds the universal value $\sigma_0 = \frac{4e^2}{\pi h}$[24,25] for ideal graphene. We have chosen here metallic ribbons, i.e., those that, when their electronic structure is computed at the simplest nearest-neighbors tight-binding model, this does not present a gap for $L \to \infty$. The results do not depend either on this choice or the direction of the injected current.

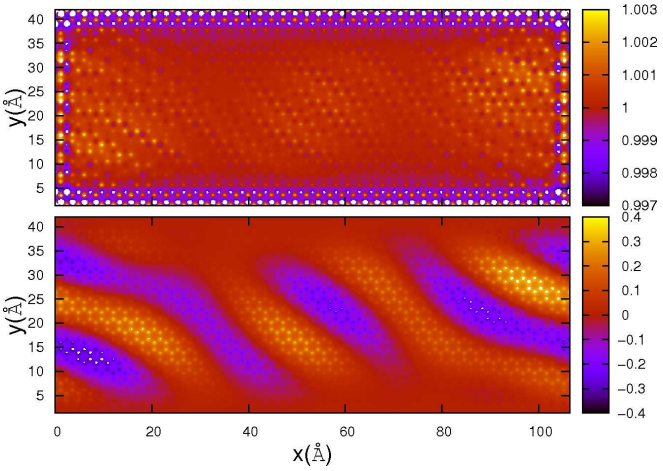

FIG. 2: Color online. Upper panel shows an example of the induced charge density due to the ripples shown in the lower panel. The scale in the upper panel refers to charge per atom which has been smoothed over a fine grid. The scale in the lower panel is given in Å.

III. POSSIBLE SOURCES OF DISORDER

We consider here two types of disorder currently accepted to possibly influence the mobility and the minimal conductivity of graphene: Charged impurities and ripples.

The model for the ripples consists of a randomly generated position-dependent height function given by the equation

$$h(x,y) = \sum_{\vec{k}}^{N_k} \frac{A\pi}{N_k|\vec{k}|} \sin\left(k_x x + k_y y\right), \qquad (1)$$

where N_k is the number of Fourier components (≈ 5) and A is the parameter that accounts for the overall deviation from planarity which is chosen as to reproduce typical ripple height-to-size ratios in the order of ≈ 0.1. $2\pi/W < k_x \ll 2\pi/a$ and $2\pi/L < k_y \ll 2\pi/a$ are random reciprocal wave vectors where a is the graphene lattice constant. Since in the hydrophene model there is only one spherical orbital per site, changes in height only affect the hopping between atoms (and the overlap), creating an accompanying pseudo-magnetic field landscape[26] which does not affect the charge density distribution. To account for changes in the on-site energies due to the sp^3 rehybridization in real graphene, we have considered a scalar potential of the type $\phi(x,y) = -B\left(\nabla^2 h(x,y)\right)^2$[27], where $B > 0$ is chosen as to reproduce potential fluctuations in the order of a few tens of meV[27]. An example of the corrugation and LDA induced charge is shown in Fig. 2.

For simplicity in the analysis of the results, we consider $Z = 1$ impurities randomly distributed in the same plane at a distance D off the hydrophene ribbon. This is probably a good assumption since charged impurities are

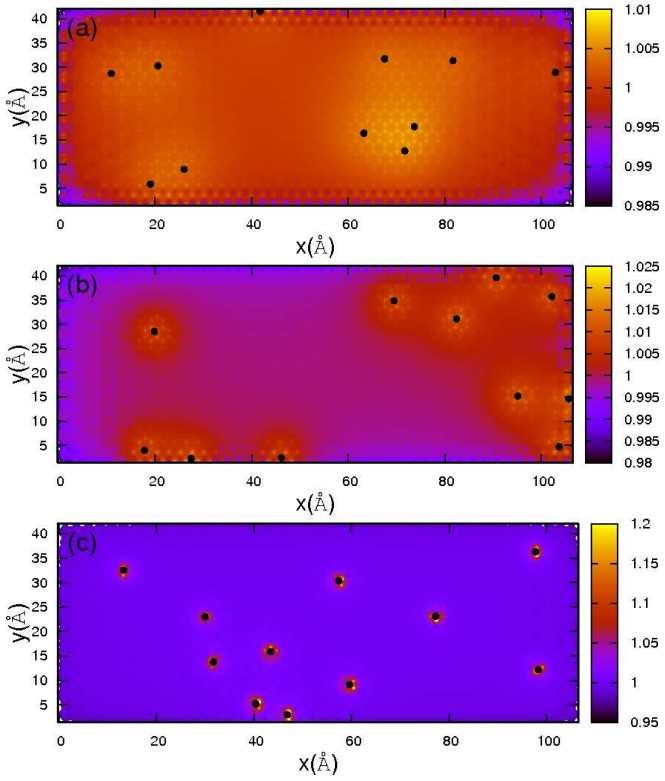

FIG. 3: Color online. Screening electron density induced by charged impurities (black dots) placed at a distance $D = 10$ (a), $D = 5$ (b), and $D = 1$ (c) Å. Overall charge neutrality within the graphene flake has been imposed in all cases. The scale refers to charge per atom which has been smoothed over a fine grid.

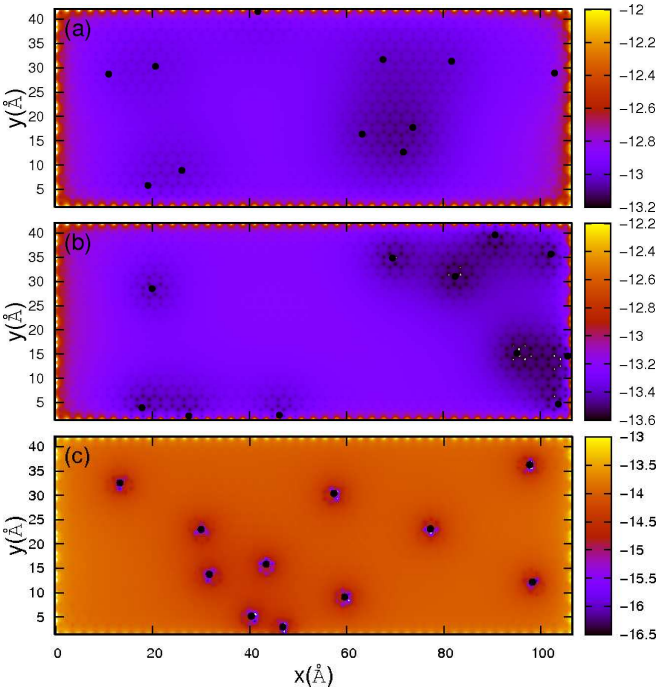

FIG. 4: Color online. Kohn-Sham potential in the graphene plane as induced by charged impurities (black dots) placed at a distance $D = 10$ (a), $D = 5$ (b), and $D = 1$ (c) Å off the graphene plane. The scale is in eV. Overall charge neutrality has been imposed in all cases within the graphene flake.

expected to be located near the surface of the SiO_2 substrate or in between the surface and the graphene flake or even adsorbed on the graphene flake, depending on their specific origin. Figure 3 shows the screening charge density for various representative disorder realizations of charged impurities at different distances off the graphene plane. Starting at $D = 10$ Å, a landscape of electron-hole puddles gives way to strongly localized screening charge around each impurity as $D \to 0$. This screening charge approaches the $\delta-$function predicted by effective models[31], although regularized by the finite value of D and by the lattice constant of our atomistic model. Figure 4 shows the accompanying Kohn-Sham potential. The range of the potential induced by a single impurity can be as small as $\xi \approx 0.5$ nm and the depth as high as 2 eV for $D = 1$ Å. which, in principle, can induce strong intervalley scattering[13]. Electron-hole puddles are also induced by the ripples due to changes in second-neighbor hopping, rehybridization, and local changes in exchange interactions[32], but the average induced electronic density is still typically one order of magnitude smaller than the one induced by impurities at $D = 10$ Å.

IV. CONDUCTIVITY RESULTS

For the conductivity calculations we have employed the code ANT.G03, which is part of the quantum transport computational toolbox ALACANT[28–30]. The basics of the calculation are as follows: i) The Bethe lattice is incorporated into the partially pre-computed Green's function of the isolated hydrophene ribbon, G_H, in the form of a self-energy Σ, ii) a density matrix is obtained from the new Green's function imposing overall charge neutrality in the ribbon, iii) a new Green's function is evaluated from the previously obtained density matrix, and iv) the procedure is repeated until a self-consistent solution is reached. For the LDA exchange correlation functional we have employed the standard approximation as implemented in GAUSSIAN03[20]. With the self-consistent Green's function and the self-energies of the left(Σ_L) and right(Σ_R) electrodes, the conductance can be calculated from the Landauer formalism:

$$G(E) = \frac{2e^2}{h} \mathrm{Tr}\left[G_H^{\dagger}(E)\Gamma_R(E)G_H(E)\Gamma_L(E)\right], \qquad (2)$$

where $\Gamma_{R(L)} = i\left(\Sigma_{R(L)} - \Sigma_{R(L)}^{\dagger}\right)$.

The LDA conductivity σ as a function of energy is presented in Fig. 5 for a ribbon with an aspect ratio $W/L \approx 3$. The length here is $L \approx 4$ nm and will remain the same in all the calculations. The solid line

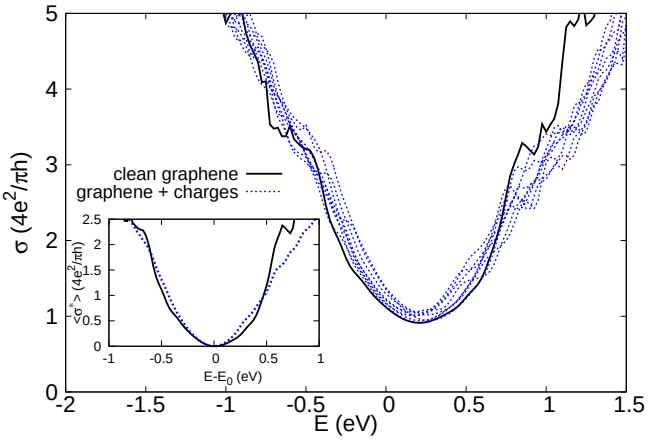

FIG. 5: Color online. Conductivity as a function of energy. The result for a clean ribbon with aspect ratio $W/L \approx 3$ is shown by the black solid line. The results for various realizations of randomly distributed impurities at a distance $D = 1$ Å corresponding to a density of $n_{\rm imp} \approx 2.0\ 10^{13}$ cm^{-2} are shown by blue dashed lines. Inset: Same as in main plot, but after averaging over disorder realizations. The minima have been offset to the origin here.

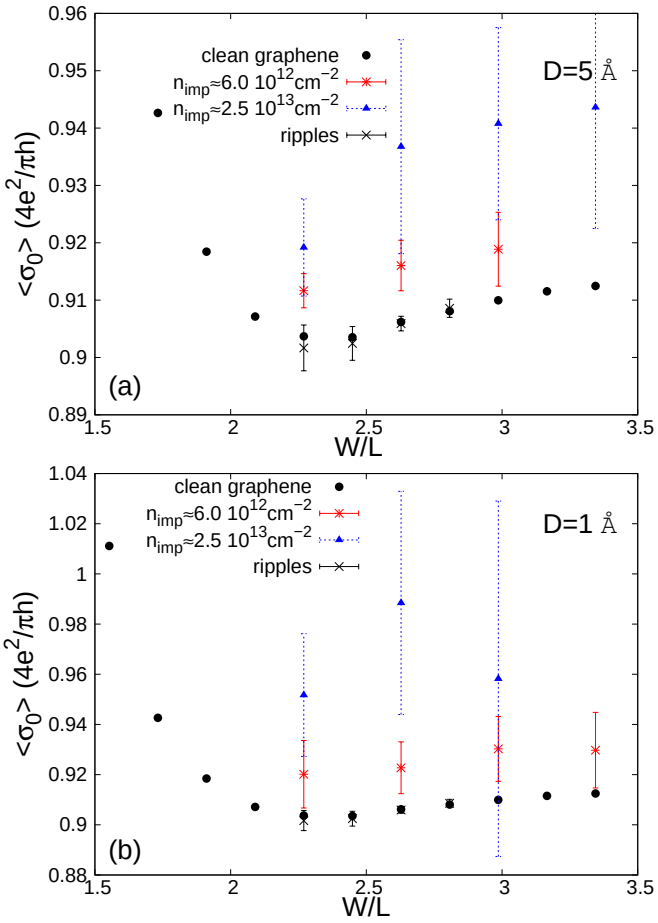

FIG. 6: Color online. Conductivity as a function of the aspect ratio. (a) The results for flat and clean graphene are represented by black dots and the ones including only ripples by crosses. The results for charged impurities placed at a distance $D = 5$ Å off the graphene plane are shown by triangles and stars for two different concentrations. (b) Same as in (a) but for a distance $D = 1$ Å.

corresponds to the ideal or "clean" case with neither ripples nor impurities. The Dirac point E_0 appears shifted to positive energies (the Fermi energy has been set to zero) due to the influence of the metallic electrodes, despite the fact that overall charge neutrality is imposed on the ribbon. We have checked, by shifting the Fermi energy upwards to the Dirac point E_0 on electron doping, that the overall conductivity curve is not appreciably affected with respect to the undoped case. From now on we will take $\sigma_0 = \sigma(E_0)$ (for E_0 typically > 0) as the minimal conductivity. This is now shown as a function of W/L (black dots) in Fig. 6. The fact that σ_0 scales with W/L to a value slightly smaller than $4e^2/\pi h$ for $W/L \to \infty$[24] can, in principle, be attributed to the chosen electrode model. One could possibly improve this result, i.e., increase the conductivity closer to the universal value $4e^2/\pi h$, by tuning the tight-binding parameters of the Bethe lattice or by using a different model for the electrodes[24,25]. Whether or not the LDA minimal conductivity of clean graphene can reach the universal value $4e^2/\pi h$ is, anyhow, not essential in the ensuing discussion.

We now turn our discussion to the effect of charged impurities and ripples on the conductivity. Figure 5 shows $\sigma(E)$ for various realizations of randomly distributed impurities at fixed $n_{\rm imp}$ and D (dashed lines). Defining $\sigma^*(E) = \sigma(E+E_0) - \sigma_0$ and averaging over impurity realizations, it becomes apparent (see inset) that $\langle\sigma^*\rangle \propto E^\alpha$ with $\alpha \approx 1$ (more visible for electrons) in contrast to the clean limit case where $\alpha > 1$. This result, in addition to our numerical evidence that the chemical potential depends linearly on the density for high values of $n_{\rm imp}$ (see also Ref. 33), provides further confirmation that $\sigma(n) \propto n$, as experimentally observed and previously explained in the Boltzmann transport approximation[14–16]. It also becomes apparent in the inset that the mobility ($\mu = \sigma/ne$) of electrons decreases as compared to that of holes[34]. All these results are nicely compatible with previous works and give us confidence on the validity of our LDA results for hydrophene.

On top of the clean graphene minimal conductivity, Fig. 6 also shows $\langle\sigma_0\rangle$ for a large set of impurity and corrugated graphene realizations for two values of D and two values of $n_{\rm imp}$. Each point has been obtained after averaging over 15-20 realizations. The results clearly indicate that, for the chosen range of D and $n_{\rm imp}$, the latter typically one order of magnitude larger than the value estimated for exfoliated graphene deposited on SiO_2 ($\approx 10^{11} - 10^{12}$ cm^2), charged impurities *increase* the minimal conductivity. Ripples, if anything, add some dispersion to the clean-limit values but their influence is negligible compared to that of charges, at least in the

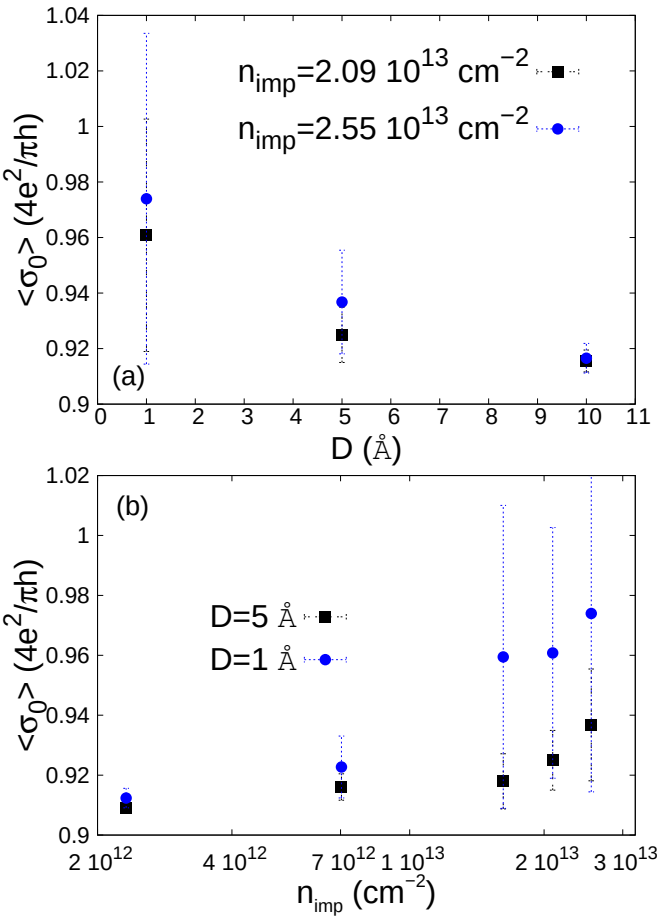

FIG. 7: Color online. Dependence of the minimal conductivity on disorder for a representative ribbon with an aspect ratio of $W/L \approx 2.6$. (a) Results for two different concentrations of charged impurities as a function of their distance to the graphene plane. (b) Results for two different distances as a function of the concentration of impurities.

range of parameters shown. Importantly, the unavoidable and large statistical uncertainty does not withstand the fact that $\langle\sigma_0\rangle$ scales to a constant value with W/L, allowing us to define a minimal conductivity for a given length L. A downward deviation is, nevertheless, apparent at large W/L for strong disorder ($D = 1$ Å) which signals the activation of localization. For completeness, we also present a systematic study of $\langle\sigma_0\rangle$ for $W/L \approx 2.6$. $\langle\sigma_0\rangle$ increases as D decreases down to the smallest meaningful value, $D = 1$ Å [see Fig. 7(a)], and increases with increasing $n_{\rm imp}$ up to the highest value considered $n_{\rm imp} \approx 2.5\,10^{13}$ cm^{-2} [see Fig. 7(b)].

A scaling analysis with L is beyond present numerical capabilities for self-consistent calculations. Nevertheless, an increasing conductivity with increasing disorder strength is compatible with the scaling law for diffusive metallic graphene in the absence of intervalley scattering[9,11,35]:

$$\sigma_0/(4e^2/h) = \frac{1}{\pi}{\rm Ln}(L/l_{\rm intra}), \qquad (3)$$

where $l_{\rm intra}$ can be interpreted as the disorder-dependent intra-valley mean free path which, in principle, can be estimated from our numerics. Notice that regardless of whether or not the weak disorder cases (large D and/or small $n_{\rm imp}$) lie outside the realm of the diffusive regime for the system sizes considered, Eq. 3 is certainly valid for the strong disorder case close to the critical value of W/L beyond which inter-valley scattering decreases the conductivity [see Fig. 6(b)]. The key observation is now that σ_0 is only increased by as much as $\approx 10\%$ with respect to the clean limit value (see Figs. 6 and 7) before localization sets in. This sets a minimum effective value for $l_{\rm intra}$ of ≈ 1.5nm with a very weak dependence on disorder over approximately a decade of (smaller) impurity concentrations and (larger) distances of the impurities to the graphene flake[36]. This minimum length can be used now to estimate the *maximum* possible value of the minimal conductivity for the experimentally largest system sizes, $\sigma_0^{\rm max}(L \approx 1\mu{\rm m}) \approx 8e^2/h$. (For larger samples L may always be effectively limited by the phase coherence length $l_\phi \lesssim 1\mu$m[37].) In summary, *the weak logarithmic L-dependence of σ_0 in Eq. 3 and the effective minimum intra-valley mean free path in the order of $\approx$ 1.5 nm combine to approximately cancel the factor π for relevant length scales ($0.1\mu m < L, l_\phi < 1\mu m$) and explain why most graphene samples exhibit minimal conductivity values in the range $8e^2/h > \sigma_0 \gtrsim 4e^2/h$.*

A few final remarks are in order. (i) For strong disorder or very large samples with unintentional disorder, i.e., for $l_{\rm inter} \ll L$, where $l_{\rm inter}$ is the inter-valley scattering length, graphene behaves as an insulator. The former condition may be achieved by intentional doping[8]. The latter, however, may be prevented by the temperature-dependent l_ϕ, which effectively limits L to $\lesssim 1\mu$m[37]. (ii) When $l_{intra} > L$, for instance, for very weak disorder or for very short samples with unintentional disorder, the scaling law in Eq. 3 for diffusive systems does no longer apply and σ_0 approaches the universal value $4e^2/\pi h$ as, e.g., reported in Refs. 1,2. (iii) Screening from the substrate or the occupied bands (not included in the model) can only increase $l_{\rm intra}$, strengthening the quasi-universal character of σ_0. (iv) Finally, when zero-energy states (or resonant states) appear due to the presence of covalently-bonded adsorbates or vacancies, a number of predictions that range from the expectation of an insulating behaviour[38] at relevant scales to a finite minimal conductivity[22] have been put forward. These, certainly, might play a role in the mobility[39] and minimal conductivity of graphene, but this study is out the scope of this work.

In summary, we have evaluated the conductivity of graphene in the presence of charge impurities and ripples including the screening in the local density approximation. Impurities are solely responsible for the increase of the minimal conductivity with respect to the clean-limit universal value. We have quantified this increase and estimated that the minimal conductivity normally lies in the range $8e^2/h > \sigma_0 \gtrsim 4e^2/h$ as observed in experi-

ments.

Acknowledgments

I appreciate discussions with A. Geim, K. Novoselov, T. Stauber, E. Prada, P. San-José, and I. Zozoulenko. This work has been financially supported by MICINN of Spain under Grants Nos. MAT07-67845 and CONSOLIDER CSD2007-00010.

[1] F. Miao, S. Wijeratne, Y. Zhang, U. C. Coskun, W. Bao, and C. N. Lau, Science **317**, 1530 (2007).

[2] R. Danneau, F. Wu, M. F. Craciun, S. Russo, M. Y. Tomi, J. Salmilehto, A. F. Morpurgo, and P. J. Hakonen, Phys. Rev. Lett. **100**, 196802 (2008).

[3] K. S. Novoselov, A. K. Geim, S. V. Morozov, D. Jiang, M. I. Katsnelson, I. V. Grigorieva, S. V. Dubonos, and A. A. Firsov, Nature **438**, 197 (2005).

[4] K. Novoselov and A. K. Geim, Nature Materials **6**, 183 (2007).

[5] Y. W. Tan, Y. Zhang, K. Bolotin, Y. Zhao, S. Adam, E. H. Hwang, S. Das Sarma, H. L. Stormer, and P. Kim, Phys. Rev. Lett. **99**, 246803 (2007).

[6] L. A. Ponomarenko, R. Yang, T. M. Mohiuddin, M. I. Katsnelson, K. S. Novoselov, S. V. Morozov, A. A. Zhukov, F. Schedin, E. W. Hill, and A. K. Geim, Phys. Rev. Lett. **102**, 206603 (2009).

[7] C. Jang, S. Adam, J. H. Chen, E. D. Williams, S. Das Sarma, and M. S. Fuhrer, Phys. Rev. Lett. **101**, 146805 (2008).

[8] J.-H. Chen, C. Jang, S. Adam, M. S. Fuhrer, E. D. Williams, and M. Ishigami, Nature Physics **4**, 377 (2008).

[9] J. H. Bardarson, J. Tworzydlo, P. W. Brouwer, and C. W. J. Beenakker, Phys. Rev. Lett. **99**, 106801 (2007).

[10] P. San-Jose, E. Prada, and D. S. Golubev, Phys. Rev. B **76**, 195445 (2007).

[11] A. Schuessler, P. M. Ostrovsky, I. V. Gornyi, and A. D. Mirlin, Phys. Rev. B **79**, 075405 (2009).

[12] C. H. Lewenkopf, E. R. Mucciolo, and A. H. Castro-Neto, Phys. Rev. B **77**, 081410(R) (2008).

[13] Y.-Y. Zhang, J. Hu, B. A. Bernevig, X. R. Wang, X. C. Xie, and W. M. Liu, Phys. Rev. Lett. **102**, 106401 (2009).

[14] S. Adam, E. H. Hwang, V. Galitski, and S. D. Sarma, Proc. Natl. Acad. Sci **104**, 18392 (2007).

[15] E. Rossi, S. Adam, and S. Das Sarma, Phys. Rev. B **79**, 245423 (2009).

[16] K. Nomura and A. H. MacDonald, Phys. Rev. Lett. **98**, 076602 (2007).

[17] M. Polini, A. Tomadin, R. Asgari, and A. H. MacDonald, Phys. Rev. B **78**, 115426 (2008).

[18] S. Adam, P. W. Brouwer, and S. Das Sarma, Phys. Rev. B **79**, 201404(R) (2009).

[19] E. Rossi, J. H. Bardarson, P. W. Brouwer, and S. Das Sarma, Phys. Rev. B **81**, 121408(R) (2010).

[20] M. J. Frisch, G. W. Trucks, H. B. Schlegel, G. E. Scuseria, M. A. Robb, J. R. Cheeseman, J. A. Montgomery, J. , T. Vreven, K. N. Kudin, et al. (2003), URL `Gaussian03,RevisionB.01,Gaussian,Inc.,PittsburghPA,2003.`

[21] A. Cortijo and M. A. H. Vozmediano, Phys. Rev. B **79**, 184205 (2009).

[22] T. Stauber, N. M. R. Peres, and F. Guinea, Phys. Rev. B **76**, 205423 (2007).

[23] M. M. Fogler, Phys. Rev. Lett. **103**, 236801 (2009).

[24] J. Tworzydlo, B. Trauzettel, M. Titov, A. Rycerz, and C. W. J. Beenakker, Phys. Rev. Lett. **96**, 246802 (2006).

[25] L. Brey, H. A. Fertig, and S. Das Sarma, Phys. Rev. Lett. **99**, 116802 (2007).

[26] F. Guinea, A. K. Geim, M. I. Katsnelson, and K. S. Novoselov, Phys. Rev. B **81**, 035408 (2010).

[27] E.-A. Kim and A. H. C. Neto, Europhysics Lett. **84**, 57007 (2008).

[28] J. J. Palacios, A. J. Pérez-Jiménez, E. Louis, and J. A. Vergés, Phys. Rev. B **64**, 115411 (2001).

[29] J. J. Palacios, A. J. Pérez-Jiménez, E. Louis, E. SanFabián, and J. A. Vergés, Phys. Rev. B **66**, 035322 (2002).

[30] J. J. Palacios, D. Jacob, A. J. Pérez-Jiménez, E. S. Fabián, E. Louis, and J. A. Vergés, *ALACANT quantum transport toolbox*, URL `http://alacant.dfa.ua.es`.

[31] A. V. Shytov, M. I. Katsnelson, and L. S. Levitov, Phys. Rev. Lett. **99**, 236801 (2007).

[32] L. Brey and J. J. Palacios, Phys. Rev. B **77**, 041403(R) (2008).

[33] E. Rossi and S. Das Sarma, Phys. Rev. Lett. **101**, 166803 (2008).

[34] D. S. Novikov, Applied Physics Lett. **91**, 102102 (2007).

[35] J. Tworzydlo, C. W. Groth, and C. W. J. Beenakker, Phys. Rev. B **78**, 235438 (2008).

[36] Although the exact range of validity of Eq. 3 is difficult to ascertain, one possibility is to compute the dimensionless parameter K_0 (see, e.g., Ref. 12), which encondes the strength of the disorder for long range models. We have obtained values in the range 1-40 which places us, for strong disorder, well into the diffusive regime for scales as short as $L = 4$nm and, for weak disorder, in the quasi-ballistic regime (see Ref. 9).

[37] D.-K. Ki, D. Jeong, J.-H. Choi, H.-J. Lee,and K.-S. Park, Phys. Rev. B **78**, 125409 (2008).

[38] J. P. Robinson, H. Schomerus, L. Oroszlany, and V. I. Falko, Phys. Rev. Lett. **101**, 196803 (2008).

[39] Z. H. Ni, L. A. Ponomarenko, R. R. Nair, R. Yang, R. S. Anissimova, I. V. Grigorieva, F. Schedin, Z. X. Shen, E. H. Hill, K. S. Novoselov, A. K. Geim, arXiv:1003.0202 (2010).